Reduction of hafnium(IV) complexes in the presence of molecular nitrogen: Attempts to form dinitrogen complexes of the heaviest group 4 element[1]

Michael D. Fryzuk, James R. Corkin, and Brian O. Patrick

Abstract: The reaction of $[P_2N_2]Li_2(dioxane)_2$ with $HfCl_4(THF)_2$ (where $[P_2N_2]$ = $PhP(CH_2SiMe_2NSiMe_2CH_2)_2PPh$) results in the formation of the hafnium dichloride complex $[P_2N_2]HfCl_2$ (**1**). The behaviour of **1** as a potential precursor in the generation of a dinitrogen coordination complex is described. Reduction of **1** with potassium-graphite (C_8K), under dinitrogen, under a variety of conditions led to a number of products, one of which is the dinuclear derivative with bridging P-phenyl groups that has the general formula $\{[P_2N_2]Hf\}_2$ (**2**). Reduction of the hafnium diiodide $[P_2N_2]HfI_2$ (**3**) — prepared via the reaction of **1** with excess Me_3SiI — with C_8K results in the formation of $([P_2N_2]Hf)_2(\mu\text{-}\eta^2\text{:}\eta^2\text{-}N_2)$ (**4**) as the major product of the reaction, while $\{[P_2N_2]Hf\}_2$ (**2**) and $[P_2N_2]Hf(C_7H_8)$ (**5**) appear to be minor products. Reaction of **1** with 2 equiv of MeMgCl gives $[P_2N_2]HfMe_2$ (**6**), which, upon exposure to an atmosphere of H_2, gives the hafnium tetrahydride $\{[P_2N_2]Hf\}_2(m\text{-}H)_4$ (**7**).

Key words: hafnium, dinitrogen, reduction, coordination chemistry, hydride, mixed donor ligands.

Résumé : La réaction du $[P_2N_2]Li_2(dioxane)_2$ avec le $HfCl_4(THF)_2$ {dans lequel $[P_2N_2]$ = $PhP(CH_2SiMe_2NSiMe_2CH_2)_2PPh$} conduit à la formation du complexe de dichlorure d'hafnium, $[P_2N_2]HfCl_2$ (**1**). On décrit le comportement du complexe **1** comme précurseur potentiel pour générer un complexe de coordination du diazote. La déduction de **1** à l'aide de potassium sur graphite (C_8K), sous atmosphère de diazote, dans diverses conditions expérimentales conduit à la formation d'un certain nombre de produits, dont l'un est un dérivé dinucléaire de formule générale $\{[P_2N_2]Hf\}_2$ (**2**) portant des groupes P-phényles agissant comme ponts. La réduction par le C_8K du complexe de diiodure d'hafnium, $[P_2N_2]HfI_2$ (**3**), préparé par le biais d'une réaction de **1** avec un excès de Me_3SiI, conduit à la formation du complexe $\{([P_2N_2]Hf)_2(\mu\text{-}\eta^2\text{:}\eta^2\text{-}N_2)$ (**4**) comme produit majeur de la réaction alors qu'il semble y avoir formation $\{[P_2N_2]Hf\}_2$ (**2**) et de $[P_2N_2]Hf(C_7H_8)$ (**5**) comme sous-produits. La réaction de **1** avec deux équivalents de MeMgCl conduit à la formation de $[P_2N_2]HfMe_2$ (**6**) qui, mis dans une atmosphère de H_2, fournit le tétrahydrure d'hafnium, $\{[P_2N_2]Hf\}_2(\mu\text{-}H)_4$ (**7**).

Mots clés : hafnium, diazote, réduction, chimie de coordination, hydrure, ligands donneurs fixés.

[Traduit par la Rédaction]

Introduction

The preparation of dinitrogen complexes of the early transition metals generally involves reduction of some suitable metal halide precursor in the presence of molecular nitrogen (1). While effective in many cases, certain early transition elements are not easily reduced, and as such, well-defined dinitrogen complexes are either unknown or extremely rare. Examples of this are the group 3 elements, Sc, Y, and La, for which molecular dinitrogen complexes are not known and the group 4 element, Hf, for which only one dinitrogen complex has been reported (2). Reduction of $Cp^*_2HfI_2$ with Na–K in dimethoxyethane at –40 °C does result in the formation of $[Cp^*_2Hf(N_2)]_2(\mu\text{-}N_2)$ in rather low yields. In this case, the choice of the reducing agent and solvent and the use of the diiodide were critical to the success of this procedure. As has been reported earlier, reductive strategies to generate dinitrogen complexes can lead to other products (3), and so, the fact that reaction optimization required considerable variation in experimental conditions is not surprising.

In this paper we describe our efforts to extend the family of hafnium dinitrogen complexes by the attempted preparation of $([P_2N_2]Hf)_2(\mu\text{-}\eta^2\text{-}N_2)$ (**4**), in analogy to that reported previously for the zirconium complex $([P_2N_2]Zr)_2(\mu\text{-}\eta^2\text{-}N_2)$. The zirconium complex has been shown to add H_2 and primary silanes with concomitant formation of N—H and N—Si bonds, respectively (4). We reasoned that access to the hafnium dinitrogen complex congener might allow for similar reactivity and even perhaps different reactivity patterns. However, as will be shown in this work, changing the metal

Received 13 March 2003. Published on the NRC Research Press Web site at http://canjchem.nrc.ca on 11 November 2003.

Dedicated to John Harrod in celebration of his contributions to inorganic chemistry, especially early metal chemistry.

M.D. Fryzuk,[2] J.R. Corkin, and B.O. Patrick. Department of Chemistry, University of British Columbia, 2036 Main Mall, Vancouver, BC V6T 1Z1, Canada.

[1] This article is part of a Special Issue dedicated to Professor John Harrod.

[2] Corresponding author (e-mail: fryzuk@chem.ubc.ca).

doi: 10.1139/V03-161

Scheme 1. Synthesis of $[P_2N_2]HfCl_2$ (**1**).

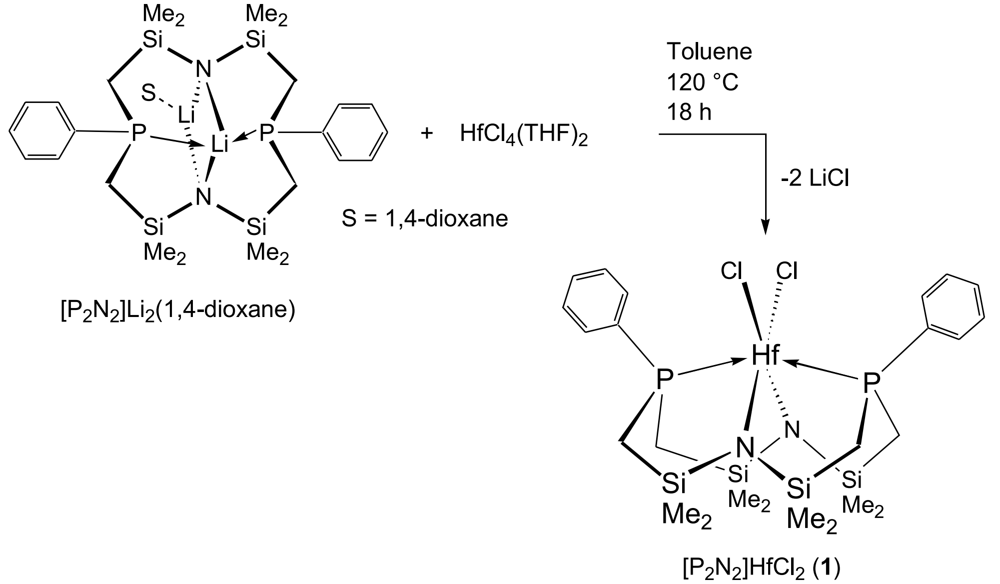

from Zr to Hf results in a different set of reactions when reduction in the presence of dinitrogen is attempted.

Results and discussion

Preparation and structure of $[P_2N_2]HfCl_2$ (1)

Our initial strategy to prepare $([P_2N_2]Hf)_2(\mu\text{-}\eta^2\text{-}N_2)$ (**4**) was to follow exactly the preparation of the zirconium analog $([P_2N_2]Zr)_2(\mu\text{-}\eta^2\text{-}N_2)$, by reduction of the Hf(IV) dichloride complex, $[P_2N_2]HfCl_2$ (**1**), with an alkali metal reagent. We have already shown that reduction of $[P_2N_2]MCl_x$ (M = Zr, x = 2; M = Nb, x = 1) by potassium-graphite (C_8K) can generate good yields of the corresponding dinitrogen complexes $([P_2N_2]M)_2(\mu\text{-}N_2)$ (M = Zr (4), M = Nb (3)). The starting dichloride **1** was prepared by the reaction of the THF adduct of hafnium(IV) tetrachloride with 1 equiv of $[P_2N_2]Li_2(1,4\text{-dioxane})_2$. The optimal conditions for this reaction were found to require heating of a suspension of starting materials in toluene overnight at approximately 120 °C (Scheme 1).

Complex **1** was characterized by solution ^1H and $^{31}P\{^1H\}$ NMR spectroscopy, elemental analysis, and solid-state, X-ray structure analysis. Crystals of **1** suitable for X-ray diffraction were grown from a saturated DME solution; the ORTEP diagram is shown in Fig. 1.

The solid-state molecular structure of **1** is best described as distorted octahedral. N(1), N(2), Cl(1), and Cl(2) can be described as forming a square plane, with the sum of the four angles equal to 360.1°. P(1) and P(2) can then be described as adopting quasi-capping positions, with a P(1)-Hf(1)-P(2) angle of 153.76(3)°, which is drawn back from the optimum 180° because of the constraints of the macrocyclic ligand framework. The small cavity size of the $[P_2N_2]$ ligand forces the hafnium atom to sit atop the ligand, which places the two chlorides *cis* to each other.

The $[P_2N_2]$ framework is distorted and adopts a C_2 twist in the solid state, a feature that has been observed in many $[P_2N_2]$ complexes (5–10). The solid-state structure of **1** is both isomorphous and isostructural with that of its zirconium analogue, $[P_2N_2]ZrCl_2$, and Table 1 shows a comparison of selected bond lengths and angles for the two compounds. As with the zirconium analogue, the Hf—N, Hf—P, and Hf—Cl bond lengths are not unusual and compare well with other group 4 amido and phosphine complexes (5, 11–13).

Like the zirconium derivative, the solid-state molecular structure of **1** does not match the solution structure. The ^1H NMR spectrum of **1** is virtually identical to that of the zirconium analogue, with slight displacements of each characteristic signal. The solution structure is more compatible with a C_{2v} symmetry. Only two signals due to the silyl methyl protons are observed, reflecting the "top and bottom" asymmetry of **1**. If the C_2 symmetry of the solid state is held in solution, one would expect to observe four silyl methyl signals. It seems, therefore, that the $[P_2N_2]$ framework is quite flexible in solution and undergoes a "rocking" motion centered at the trigonal silyl amide groups. The $^{31}P\{^1H\}$ NMR spectrum of **1** shows a singlet at –5.8 ppm, which is shifted 8.5 ppm downfield from that observed for the zirconium analogue.

Reduction of $[P_2N_2]HfCl_2$ (1)

While ease of reduction is difficult to compare, tables of reduction potentials indicate that Hf is more difficult to reduce than zirconium (14–15). The first attempt to reduce **1** followed a procedure identical to the one that formed the zirconium dinitrogen complex; it involved reduction of the starting chloride complex with 2 equiv of potassium graphite (4), but the results were unexpected. Instead of the desired dinitrogen complex, the major product was the hafnium dimer, $\{[P_2N_2]Hf\}_2$ (**2**), with coordination of the activated phenyl rings on one phosphorus to the other metal atom (Scheme 2).

The NMR spectra of **2** are consistent with this dimeric formulation. The ^1H NMR spectrum shows a set of phosphorus–phenyl resonances in a 2:2:1 ratio at 4.22, 4.15, and 3.39 ppm, respectively. Coupling information is transmitted through the coordinated arene ring between metal centers,

Fig. 1. An ORTEP diagram of $[P_2N_2]HfCl_2$ (**1**), showing the solid-state molecular structure (ellipsoids at 50% probability). The silyl methyl groups have been omitted for clarity; only the *ipso* carbons of the phosphorus phenyl groups are shown.

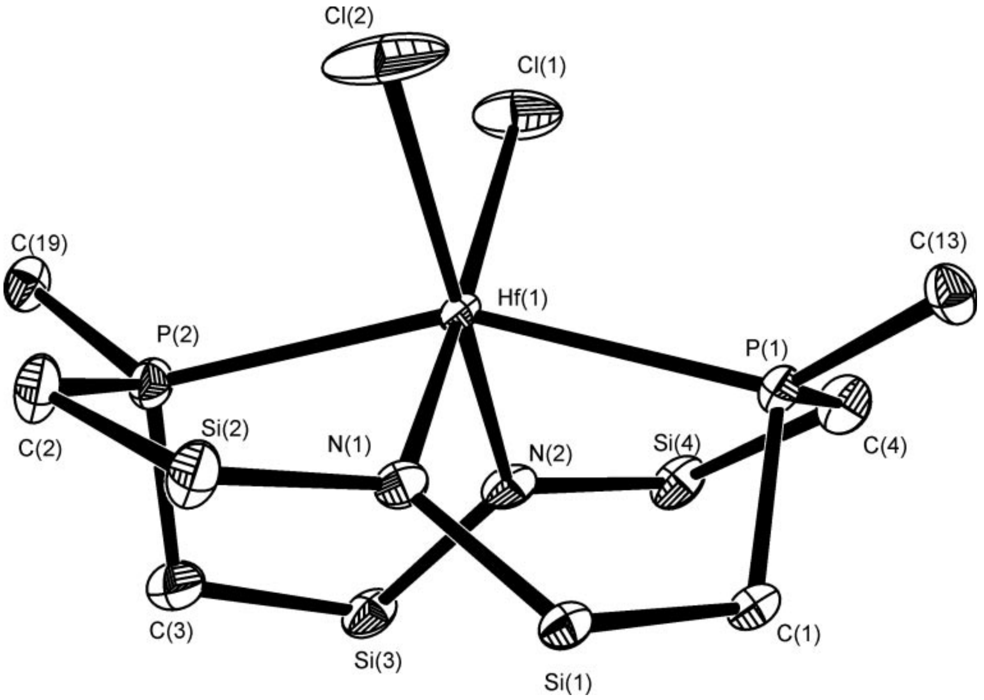

Table 1. A comparison of selected bond lengths (Å) and angles (°) in $[P_2N_2]MCl_2$ (M = Zr, Hf).

Bond lengths	M = Hf	M = Zr	Bond angles	M = Hf	M = Zr
M(1)—N(1)	2.125(3)	2.136(4)	N(1)-M(1)-N(2)	96.6(1)	96.8(2)
M(1)—N(2)	2.134(3)	2.125(4)	P(1)-M(1)-P(2)	153.76(3)	152.52(6)
M(1)—P(1)	2.684(1)	2.694(2)	Cl(1)-M(1)-Cl(2)	83.32(4)	82.57(7)
M(1)—P(2)	2.673(1)	2.707(2)	N(1)-M(1)-Cl(2)	90.88(9)	89.5(1)
M(1)—Cl(1)	2.461(1)	2.455(2)	N(2)-M(1)-Cl(1)	89.22(9)	91.3(1)
M(1)—Cl(2)	2.461(1)	2.448(2)			

leading to an AA′BB′ pattern in the $^{31}P\{^1H\}$ NMR spectrum. This compound also has a zirconium analogue, $\{[P_2N_2]Zr\}_2$, which is the major product when $[P_2N_2]ZrCl_2$ is reduced with C_8K in the absence of N_2, for example, under Ar or in a degassed vessel (3). $\{[P_2N_2]Zr\}_2$ was first noticed as an impurity in the reaction that produces $\{[P_2N_2]Zr\}(\mu\text{-}\eta^2\text{:}\eta^2\text{-}N_2)$. For the zirconium system, under N_2, the dimer was a fairly minor impurity. When the metal center is changed to hafnium, the dimer appears to be the major product of this reaction, at least under these conditions.

Preparation and reduction of $[P_2N_2]HfI_2$ (3)

The only known hafnium dinitrogen complex, $\{Cp^*{}_2Hf(N_2)\}_2(\mu\text{-}N_2)$, was prepared from the precursor, $Cp^*{}_2HfI_2$, after attempts to use a dichloride complex as a starting material were unsuccessful (2). Reaction of a toluene solution of $[P_2N_2]HfCl_2$ (**1**) with a slight excess of trimethylsilyliodide resulted in formation of $[P_2N_2]HfI_2$ (**3**) (Scheme 3).

Assuming an analogous structure for the diiodide as was found for the dichloride, one would expect little change in the NMR spectra upon replacement of chloride with iodide, and to a degree this is observed. The $^{31}P\{^1H\}$ NMR signal is still a singlet at –5.4 ppm, shifted only 0.4 ppm downfield of the dichloride **2**. In the ^1H NMR spectrum of the diiodide complex, the two silyl methyl signals are now separated by 0.3 ppm, while for the dichloride complex the separation is less than 0.05 ppm.

Reaction of $[P_2N_2]HfI_2$ (**3**) with 2 equiv of C_8K under 1 atm (1 atm = 101.325 kPa) of dinitrogen produced a mixture of products and a solution with an intense blue color, a color characteristic of the $\{[P_2N_2]Zr\}(\mu\text{-}\eta^2\text{:}\eta^2\text{-}N_2)$ analogue. These products, their tentative assignments, and their percentages as determined by $^{31}P\{^1H\}$ NMR spectroscopy are summarized in Table 2.

The $^{31}P\{^1H\}$ NMR chemical shift of the speculated dinitrogen complex, combined with the intense blue color of the solution, was an excellent indication of dinitrogen complex formation, but it remained uncertain that the signal at –8.2 ppm could be assigned to $\{[P_2N_2]Hf\}(\mu\text{-}\eta^2\text{:}\eta^2\text{-}N_2)$.

In an attempt to increase the yield of the dinitrogen complex **4**, the reaction was repeated in a sealed reactor, under 4 atm of dinitrogen, for a period of 8 days (Table 3). With these changes in reaction conditions, the signal at –8.2 ppm became the major signal. The large increase in integration size of this signal, when the only change to the reaction was to increase the N_2 pressure, is further evidence that the signal can be assigned to the dinitrogen complex. However, a

Scheme 2. Synthesis of $\{[P_2N_2]Hf\}_2$ (**2**).

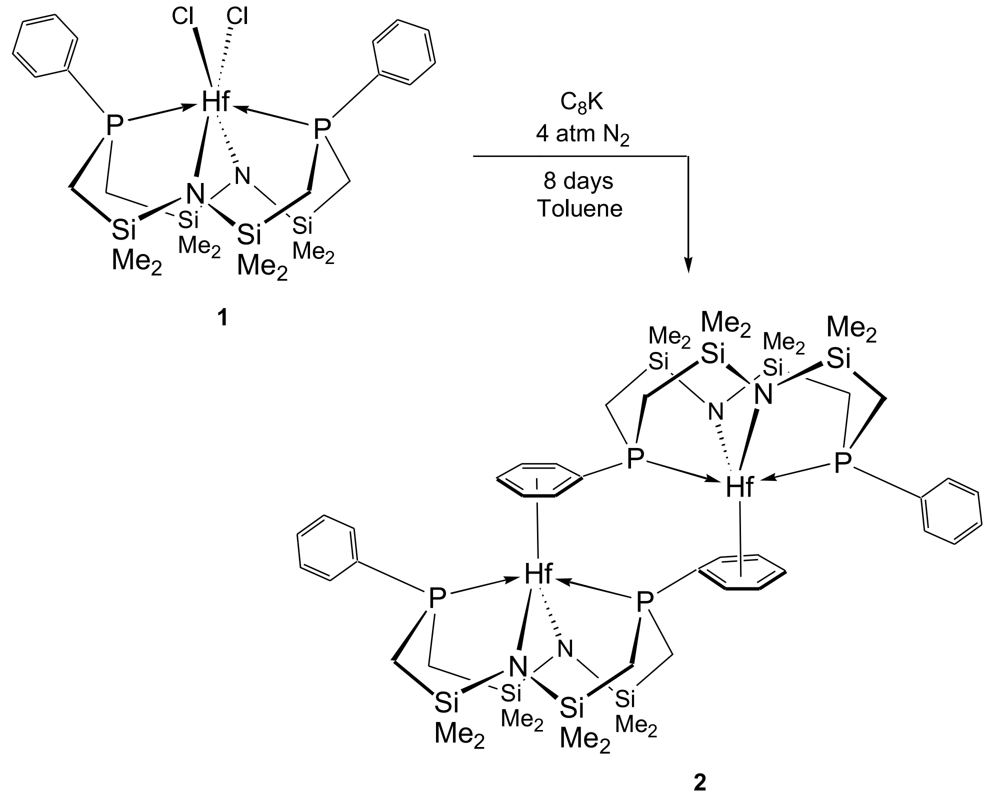

Scheme 3. Synthesis of $[P_2N_2]HfI_2$ (**3**).

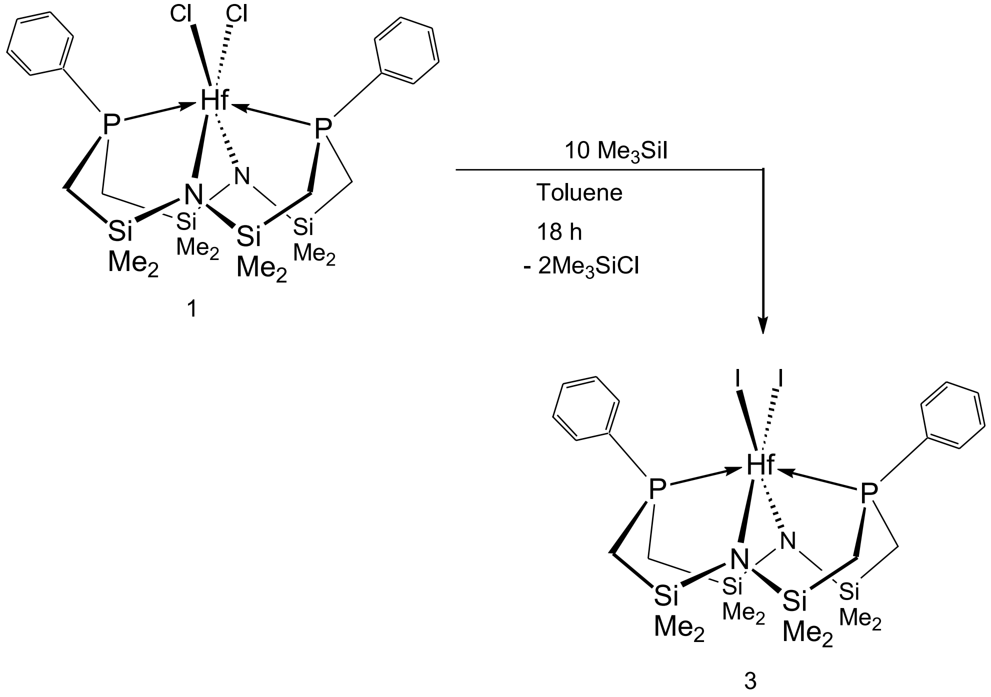

higher percentage of starting material remains when compared with the same reaction using 1 atm of N_2, and the other impurities are still present, although in smaller amounts.

Further characterization of $\{[P_2N_2]Hf\}_2(\mu\text{-}\eta^2\text{:}\eta^2\text{-}N_2)$ (4)

Further evidence for the formation of complex **4** comes from mass spectrometry data. Shown in Fig. 2 is a portion of the EI mass spectrum. Figure 3 shows the theoretical mass

Table 2. The results of a study of the reaction of $[P_2N_2]HfI_2$ (**3**) with 2 equiv of C_8K under 1 atm N_2 in toluene.

Compound	^{31}P shift (ppm)	After 1 h (%)[a]	After 4 h (%)	After 8 h (%)	After 25 h (%)	After 72 h (%)
$[P_2N_2]HfI_2$ **3**	–5.4 (s)	100	77	55	31	5
$\{[P_2N_2]Hf\}_2$ **2**	6.3 (m)[b]	0	9	21	26	34
$[P_2N_2]Hf(C_7H_8)$ **5**	8.6 (s)	0	8	14	22	33
$\{[P_2N_2]Hf\}_2(\mu\text{-}N_2)$ **4**	–8.2 (s)	0	6	9	21	29

[a] Percentages of each compound determined from integration of their $^{31}P\{^1H\}$ NMR signals. Error is approximately 1% for each.

[b] Spin system is AA′BB′.

Table 3. The results of a study of the reaction of $[P_2N_2]HfI_2$ (**3**) with 2 equiv of C_8K under 4 atm N_2 in toluene.

	$[P_2N_2]HfI_2$ **3**	$\{[P_2N_2]Hf\}_2$ **2**	$[P_2N_2]Hf(C_7H_8)$ **5**	$\{[P_2N_2]Hf\}_2(\mu\text{-}N_2)$ **4**
^{31}P shift (ppm)	–5.4 (s)	6.3 (m)[a]	8.6 (s)	–8.2 (s)
After 8 days under 4 atm N_2 (%)[b]	19	16	13	52

[a] Spin system is AA′BB′.

[b] Percentages of each compound determined from integration of their $^{31}P\{^1H\}$ NMR signals. Error is approximately 1% for each.

Fig. 2. Selected EI mass spectrometry data for $([P_2N_2]Hf)_2N_2$ (**4**).

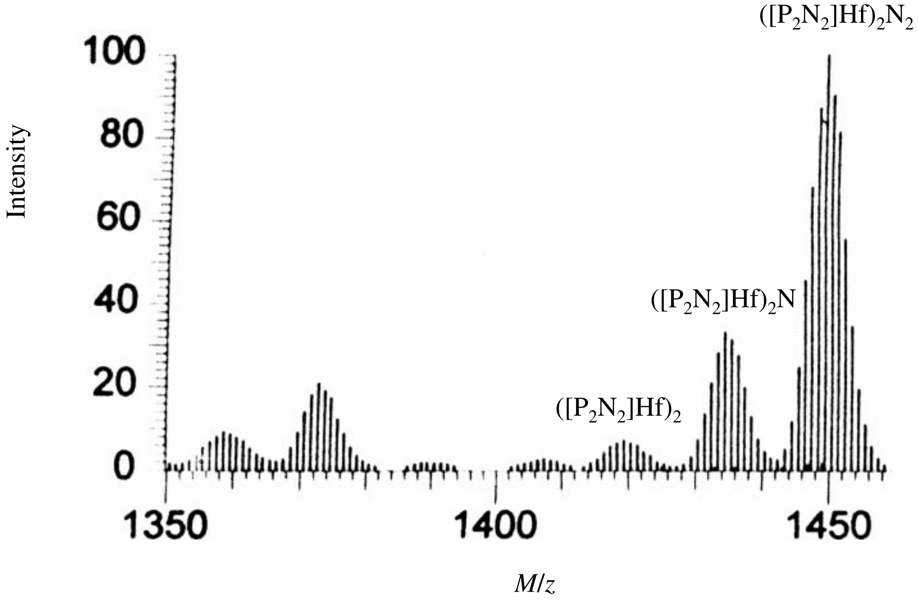

Fig. 3. Theoretical isotope distribution pattern for EI mass spectrometry analysis of $([P_2N_2]Hf)_2N_2$ (**4**), as determined by Isotope Pattern Calculator™ v. 1.6.6.

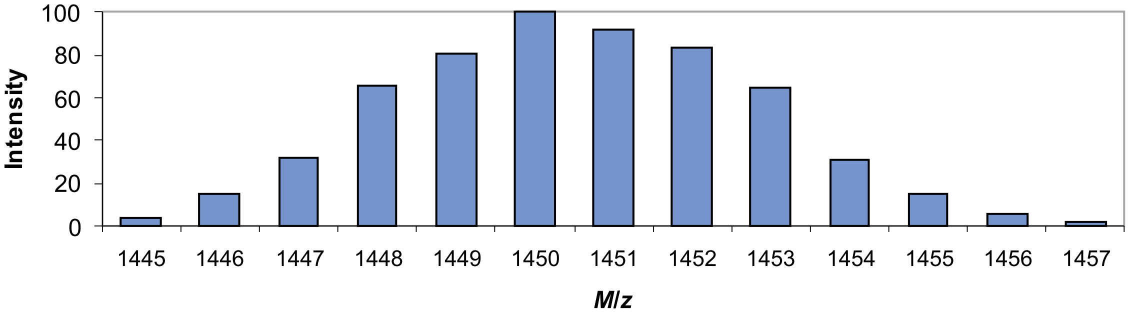

spectrometry signature one would expect from complex **4**. The theoretical signature is a near exact match for the experimental one shown in Fig. 2. In Fig. 2, signatures for $\{[P_2N_2]Hf\}_2N$ (where a single nitrogen atom has been stripped from the parent compound) and for $\{[P_2N_2]Hf\}_2$ (**2**) can also be seen and are labeled.

Not shown here, but also observed in the EI mass spectrum, are the signatures for $[P_2N_2]Hf(C_7H_8)$ (**5**) and for

Scheme 4. Synthesis of $[P_2N_2]HfMe_2$ (**6**).

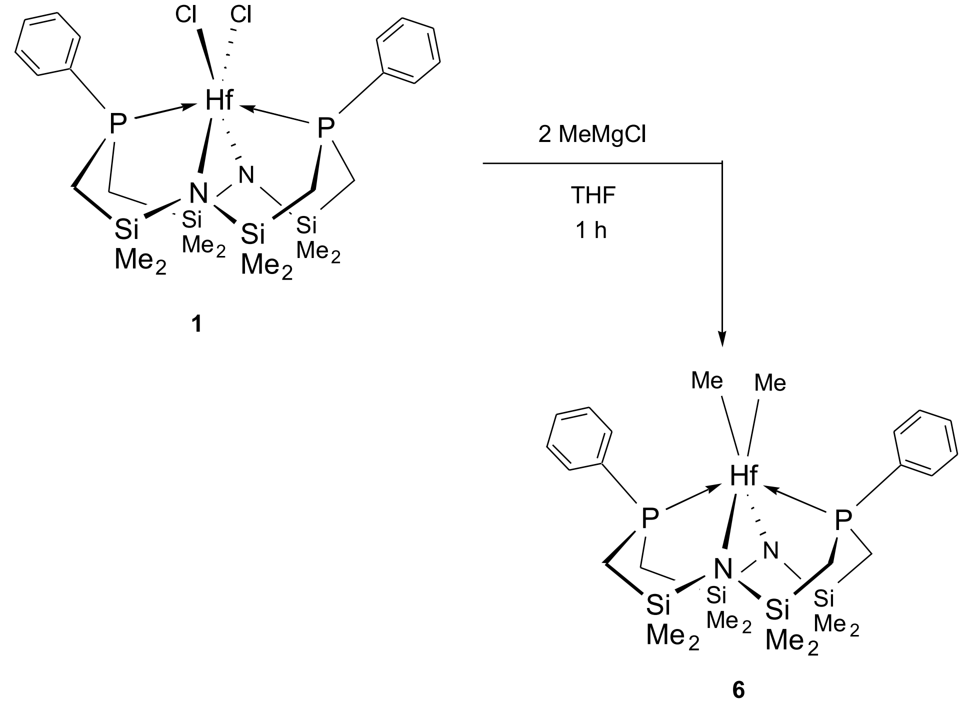

$[P_2N_2]HfI$ and $[P_2N_2]Hf$. Interestingly, no signature is observed for $[P_2N_2]HfI_2$ (**3**), likely because of the weakness of the Hf—I bond.

To confirm the presence of a dinitrogen compound in the products from the reaction of $[P_2N_2]HfI_2$ (**3**) with 2 equiv of C_8K, the mixture of products was degraded with HCl and the resultant products analyzed to detect hydrazine, according to literature procedure (16). Hydrazine was detected, confirming the presence of a dinitrogen compound; however, it was not possible to determine the percent of hydrazine formed per mole of $\{[P_2N_2]Hf\}_2(\mu\text{-}\eta^2{:}\eta^2\text{-}N_2)$ (**4**), owing to the inability to isolate **4** in pure form.

Preparation and structure of $[P_2N_2]HfMe_2$ (6)

We were also interested in the organometallic chemistry of hafnium with the $[P_2N_2]$ ligand. $\{[P_2N_2]Zr\}_2(\mu\text{-}H)_4$ was prepared[3] from $[P_2N_2]ZrCl_2$, using C_8K as a reducing agent, under 4 atm of H_2. Interestingly, it does not appear to be possible to form a zirconium hydride from $[P_2N_2]ZrMe_2$. $[P_2N_2]ZrMe_2$ is extremely thermally and light sensitive, making it difficult to prepare in sufficient quantities to use in subsequent reactions. It is a well-established precedent that certain organometallic hafnium(IV) compounds are more thermally stable than their zirconium analogues (12, 17–19). As well, the use of hafnium analogues can facilitate investigation of intermediates in cases where this proves difficult for zirconium compounds (2, 20, 21). The synthesis of $[P_2N_2]HfMe_2$ (**6**) was accomplished by the metathesis reaction of $[P_2N_2]HfCl_2$ (**1**) with 2 equiv of the Grignard reagent, MeMgCl (Scheme 4).

Compound **6** was characterized by ^1H and $^{31}P\{^1H\}$ NMR spectroscopy, elemental analysis, and X-ray crystal structure analysis. In a manner similar to most other known mononuclear group 4 metal $[P_2N_2]$ complexes, the dimethyl compound adopts C_{2v} symmetry in solution at ambient temperature, as evidenced by NMR spectroscopy. As expected, the methyl protons are coupled to two equivalent phosphorus nuclei and appear as a triplet at 0.65 ppm. Unlike the case of the zirconium analogue, their signal is not masked by the $[P_2N_2]$ ligand methylene protons. Interestingly, while it was not possible to grow crystals of the zirconium analogue of this compound, crystals of the hafnium analogue were grown easily from slow evaporation of a DME solution. An ORTEP diagram of complex **6** is shown in Fig. 4. The substitution of methyl groups for chloride moieties upon going from **1** to **6** has resulted in a substantial structural change. The geometry around the metal center is now best described as trigonal prismatic, with the two trigonal planes described by N(1), P(1), and C(25) and N(2), P(2), and C(26). The methyl carbons are not located in a square plane with the amido nitrogens but are rotated out of this plane. As well, the phosphine and amide "bite angles", P(1)-Hf-P(2) and N(1)-Hf-N(2), have both changed considerably. The phosphine bite angle has decreased from 153.76(3)° to 135.79(3)°, while the amide bite angle has increased from 96.6(1)° to 113.2(1)°. Table 4 shows selected bond distances and angles for complex **6**. The Hf—C, Hf—N, and Hf—P bond distances are, once again, not unusual and compare well with other group 4 methyl complexes (11).

Preparation of $\{[P_2N_2]Hf\}(\mu\text{-}H)_4$ (7)

While hydrogenolysis of $[P_2N_2]ZrMe_2$ did not result in a zirconium hydride complex, a hafnium hydride was synthesized through hydrogenolysis. Reaction of $P_2N_2HfMe_2$ with H_2 gas in benzene gave $\{[P_2N_2]Hf\}_2(\mu\text{-}H)_4$ **7** (Scheme 5). Complex **7** is sparingly soluble in benzene and precipitates

---

[3] M.D. Fryzuk and J.B. Love. Unpublished results.

Fig. 4. An ORTEP diagram showing the solid-state molecular structure of $[P_2N_2]HfMe_2$ (**6**) (ellipsoids at 50% probability). The silyl methyl groups have been omitted for clarity; only the *ipso* carbons of the phosphorus phenyl groups are shown.

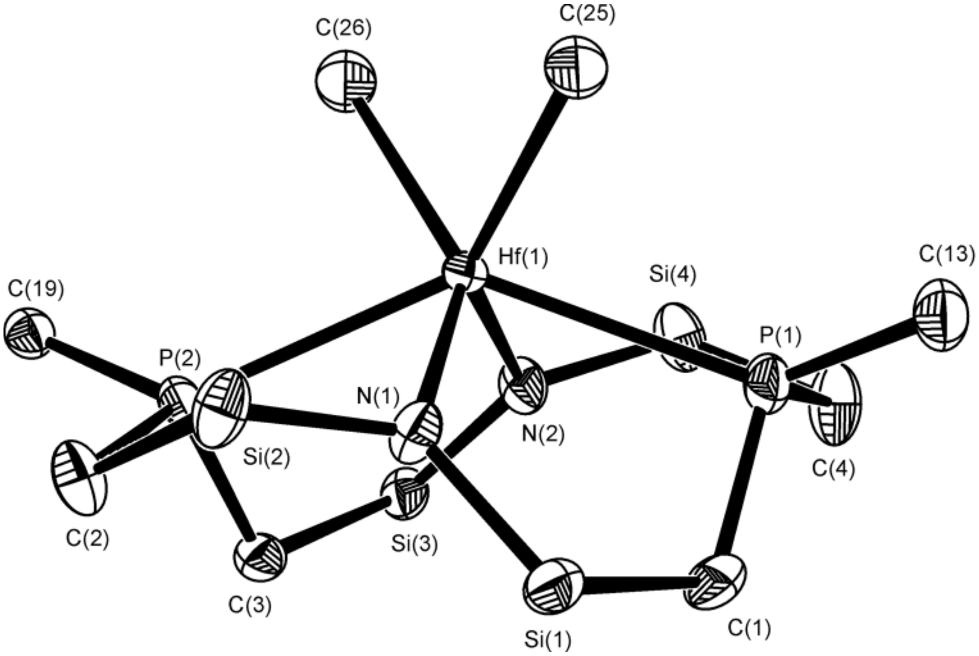

Table 4. Selected bond lengths (Å) and angles (°) in $[P_2N_2]HfMe_2$ (**6**).

Bond lengths		Bond angles	
Hf(1)—N(1)	2.147(3)	N(1)-Hf(1)-N(2)	113.5(1)
Hf(1)—N(2)	2.149(3)	P(1)-Hf(1)-P(2)	135.79(3)
Hf(1)—P(1)	2.781(1)	C(25)-Hf(1)-C(26)	82.0(2)
Hf(1)—P(2)	2.783(1)	N(1)-Hf(1)-C(25)	97.2(2)
Hf(1)—C(25)	2.263(1)	N(2)-Hf(1)-C(25)	134.6(2)
Hf(1)—C(26)	2.277(1)		

out of solution as yellow microcrystals, making separation from the parent compound a simple matter.

The change in the chemical shift of the phosphorus nuclei, when switching from $\{[P_2N_2]Zr\}_2(\mu\text{-}H)_4$ to its hafnium analogue,[3] is more drastic than in other $[P_2N_2]$ compounds. The signal is observed at 4.4 ppm, downfield from the zirconium analogue signal at –5.9 ppm. As well, the hydride quintet (2, 22–24) is observed at 9.3 ppm, downfield from 5.0 ppm in the zirconium analogue. The other characteristic signals in the ^1H NMR spectrum have not changed appreciably.

Conclusions

The hafnium chemistry presented in this paper, while similar to the previously reported zirconium chemistry, does have some notable differences. Although the X-ray crystal structure of $[P_2N_2]HfCl_2$ (**1**) is isostructural and isomorphous with that of its zirconium analogue, the reactivity of **1**, especially under reducing conditions, is quite different. It was not possible to synthesize the hafnium dinitrogen compound $\{[P_2N_2]Hf\}(\mu\text{-}\eta^2\text{:}\eta^2\text{-}N_2)$, in any appreciable amount, from $[P_2N_2]HfCl_2$ (**1**); instead, a hafnium dimer, $\{[P_2N_2]Hf\}_2$ (**2**), was the major product. However, changing the hafnium starting material from the chloride complex, **1**, to the iodide complex did result in the formation of the hafnium dinitrogen complex, $\{[P_2N_2]Hf\}(\mu\text{-}\eta^2\text{:}\eta^2\text{-}N_2)$ (**4**), after reduction with C_8K, as shown by NMR spectroscopy, EI mass spectrometry, and hydrazine analysis. Unfortunately, it has not been possible to isolate compound **4** in the solid state. Synthesis of $[P_2N_2]HfMe_2$ (**6**) proceeded in a manner identical to that of its zirconium analogue. The dimethyl derivative, **6**, reacts with H_2 to generate the dinuclear hafnium hydride, $\{[P_2N_2]Hf\}(\mu\text{-}H)_4$ (**7**), via hydrogenolysis; this reaction fails for the zirconium analogue, $[P_2N_2]ZrMe_2$.

Experimental

Materials and apparatus

All manipulations were performed under prepurified nitrogen in a Vacuum Atmospheres HE-553-2 workstation equipped with an MO-40-2H purification system or using Schlenk-type glassware. The term “reactor” refers to a cylindrical, thick-walled Pyrex vessel equipped with a 5 mm (or 10 mm, for larger bombs) Kontes teflon needle valve and a ground glass joint for attachment to a vacuum line. These “reactors” allow pressures as high as 4 atm to be maintained inside the tube. $HfCl_4$ (<0.05% Zr) was purchased from Strem and used as received. THF was predried by refluxing over CaH_2 for at least 24 h and dried by refluxing over sodium benzephenone ketyl, followed by distillation under argon. Toluene and hexanes were purchased in anhydrous form from Aldrich, sparged with N_2, and deoxygenated by filtration through columns containing silica and Q-5 catalyst under a positive pressure of N_2 (25). Benzene, diethyl ether, and dimethoxyethane were also refluxed over sodium benzephenone ketyl and distilled under argon. Deuterated THF (C_4D_8O) and deuterated benzene (C_6D_6) were refluxed under vacuum with sodium–potassium amalgam (Na–K),

Scheme 5. Synthesis of $\{[P_2N_2]Hf\}_2(\mu\text{-}H)_4$ (**7**).

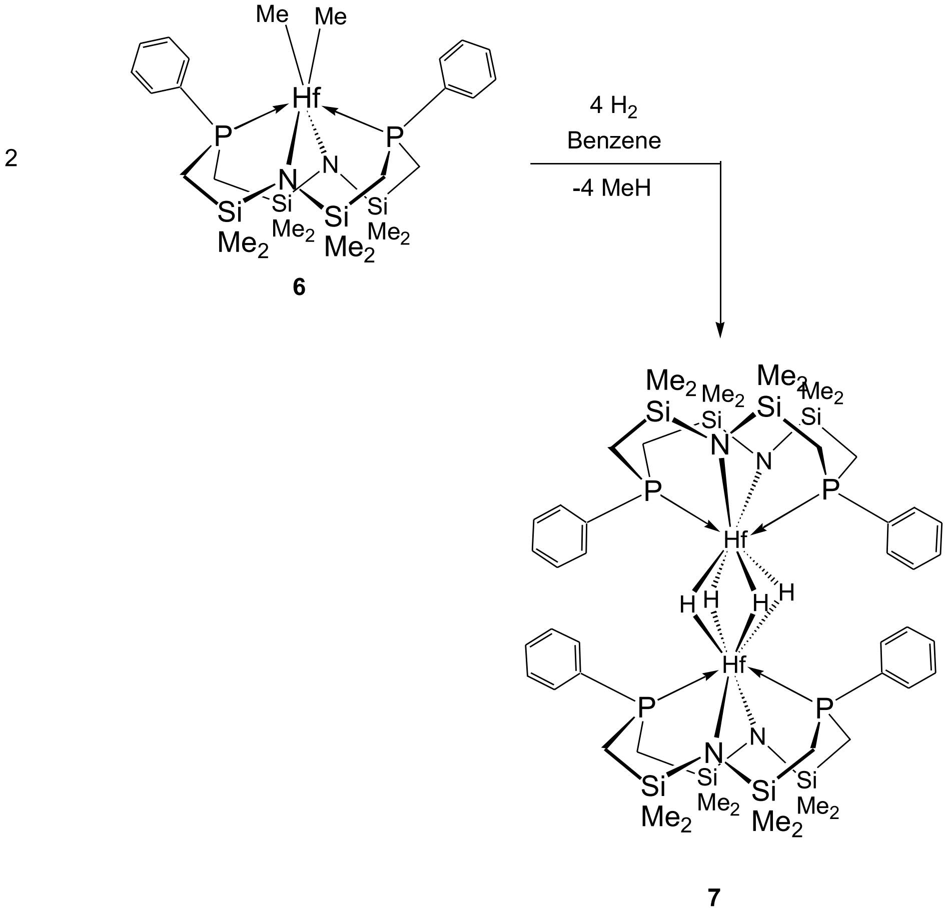

vacuum transferred to a clean vessel, and "freeze–pump–thawed" three times prior to use.

The following compounds were prepared by published procedures: $HfCl_4(THF)_2$ (26), [*syn*-P_2N_2]Li_2(dioxane) (27), C_8K (28), and $Mg(C_4H_6)(THF)_2$. Me_3SiI, MeMgCl, BzMgCl, and H_2 were used as received. Diatomaceous earth (Celite) was dried overnight at 170 °C before being taken inside the glovebox for use.

Analytical methods

^1H and $^{31}P\{^1H\}$ NMR spectroscopy were performed on a Bruker AMX-500 instrument (500.135 and 202.458 MHz) or a Bruker AC-200 machine (200.132 and 81.015 MHz). ^1H NMR spectra were referenced to internal C_6D_5H (7.15 ppm), and $^{31}P\{^1H\}$ NMR spectra were referenced to external $P(OMe_3)_3$ (141.0 ppm, with respect to 85% H_3PO_4 at 0.00 ppm).

The theoretical EI signature was created using Isotope™ v. 1.6.6, a program designed specifically to model mass spectrometry signatures.

C, H, and N microanalyses were performed by Mr. P. Borda of this department, the Department of Chemistry, University of British Colombia (UBC). The X-ray crystal structures were determined at UBC Crystallographic Services in this department by Dr. B. Patrick. The crystals were loaded in a small glass vial and covered with paratone oil in the glovebox to prevent decomposition. Details of the structure determinations are given in the Appendices.[4]

Hydrazine analysis (16)

The products from the reaction of $[P_2N_2]HfI_2$ (**3**) with 2 equiv of C_8K were weighed into a 200 mL Schlenk tube (0.280 g) and dissolved in 50 mL of Et_2O. Ten millilitres of 2.0 mol L^{-1} HCl in Et_2O was added to this solution. The solution immediately lost its blue color, and a white precipitate formed. The clear solution and white precipitate were stirred for 1 h, and the solvents were removed in vacuo. The flask was exposed to the air, extracted into 100 mL of H_2O, and filtered into a 500 mL volumetric flask, which was filled with 1.0 mol L^{-1} HCl. A 2.0 mL aliquot of this solution was added to 20 mL of a color developer (*p*-dimethylaminobenzaldehyde, 4.0 g; ethanol, 200 mL; 1.0 mol L^{-1} HCl, 20 mL) and diluted to 25.0 mL with 1.0 mol L^{-1} HCl. Absorbance readings of the sample were taken within 10 min. The spectrometer was set to 100% transmittance, using a blank solution consisting of

---

[4] Supplementary data may be purchased from the Depository of Unpublished Data, Document Delivery, CISTI, National Research Council Canada, Ottawa, ON K1A 0S2, Canada (http://www.nrc.ca/cisti/irm/unpub_e.shtml for information on ordering electronically). CCDC 205941 and 205942 contain the supplementary data for this paper. These data can be obtained, free of charge, via www.ccdc.cam.ac.uk/conts/retrieving.html (or from the Cambridge Crystallographic Data Centre, 12 Union Road, Cambridge, U.K.; fax +44 1223 336033; or deposit@ccdc.cam.ac.uk).

1.0 mol L^{-1} HCl. Absorbance readings of 0.33, 0.34, and 0.33 AU were obtained at 458 nm.

Synthesis of $[P_2N_2]HfCl_2$ (1)

$Li_2(dioxane)[P_2N_2]$ (6.83 g, 10.8 mmol) and $HfCl_4(THF)_2$ (5.00 g, 10.8 mmol) were each weighed into a thick-walled reactor. Addition of 150 mL toluene to this intimate mixture resulted in a cloudy white solution. The reactor was sealed, and the mixture was heated for 18 h at 120 °C. The solvents were then removed in vacuo; the off-white residue was extracted into toluene (2 × 50 mL) and filtered through Celite. The filtrate was evaporated to dryness and the residue washed with hexanes (2 × 10 mL), yielding **1** (7.25 g, 86%) as a white powder. The product was crystallized by the slow evaporation of a DME solution.

^1H NMR (C_6D_6, 25 °C, 500.135 MHz) δ: 7.87 (m, 4H, *o*-H phenyl), 7.05 (m, 6H, *m*/*p*-H phenyl), 1.41 (ABX m, 4H, CH_2 ring), 1.32 (ABX m, 4H, CH_2 ring), 0.38 (s, 12H, $SiMe_2$ ring), 0.34 (s, 12H, $SiMe_2$ ring). $^{31}P\{^1H\}$ (C_6D_6, 25 °C, 202.458 MHz) δ: –5.8 (s). Anal. calcd. for $C_{24}H_{42}Cl_2HfN_2P_2Si_4$: C 36.85, H 5.41, N 3.58; found: C 37.04, H 5.48, N 3.56.

Synthesis of $\{[P_2N_2]Hf\}_2$ (2)

$[P_2N_2]HfCl_2$ (**1**) (0.73 g, 0.93 mmol) and C_8K (0.25 g, 1.86 mmol) were each weighed into a 200 mL thick-walled reactor, to which 50 mL of toluene was added, all in the glovebox. The reactor was removed from the glovebox and cooled to –198 °C in a liquid nitrogen bath while under a flow of N_2. After allowing 30 min for equilibration, the reactor was sealed and allowed to warm to room temperature. The reaction mixture was stirred for 8 days and filtered through Celite. Toluene was removed in vacuo, and the residues were dissolved in hexanes and filtered. The hexanes solution was left in a –40 °C freezer overnight, where **2** crashed out of solution as a yellow-brown powder. Yield: 0.22 g, 32.2%. Note: further studies showed that it does not matter what type of atmosphere (N_2, Ar, or near vacuum) is inside the reactor.

^1H NMR (C_6D_6, 25 °C, 200.132 MHz) δ: 7.40 (m, 4H, *o*-H phenyl), 7.10 (m, 6H, *m*/*p*-H phenyl), 4.22 (m, 4H, *m*/*p*-H activated phenyl), 4.15 (m, 4H, *m*/*p*-H activated phenyl), 3.39 (m, 2H, *o*-H activated phenyl), 1.49 (ABX m, 8H, CH_2 ring), 1.15 (ABX m, 8H, CH_2 ring), 0.52 (s, 12H, $SiMe_2$ ring), 0.50 (s, 12H, $SiMe_2$ ring), 0.31 (s, 12H, $SiMe_2$ ring), 0.04 (s, 12H, $SiMe_2$ ring). $^{31}P\{^1H\}$ (C_6D_6, 25 °C, 81.015 MHz) δ: –6.3 (m). Anal. calcd. for $C_{48}H_{84}Hf_2N_4P_4Si_8$: C 40.52, H 5.95, N 3.95; found: C 40.39, H 5.97, N 3.75.

Synthesis of $[P_2N_2]HfI_2$ (3)

Me_3SiI (10.0 mL, 70 mmol, ~10 equiv) was added to a stirred solution of $[P_2N_2]HfCl_2$ (**1**) (5.21 g, 6.66 mmol) in 80 mL of toluene at –78 °C. The reactor was sealed and the solution stirred for 18 h, during which time the solution acquired a very pale yellow-green color. Toluene was removed in vacuo and the residues washed with hexanes (2 × 10 mL), yielding **3** (2.8 g, 88%) as a very pale green powder.

^1H NMR (C_6D_6, 25 °C, 200.132 MHz) δ: 7.92 (m, 4H, *o*-H phenyl), 7.05 (m, 6H, *m*/*p*-H phenyl), 1.58 (ABX m, 4H, CH_2 ring), 1.27 (ABX m, 4H, CH_2 ring), 0.48 (s, 12H, $SiMe_2$ ring), 0.39 (s, 12H, $SiMe_2$ ring). $^{31}P\{^1H\}$ (C_6D_6, 25 °C, 81.015 MHz) δ: –5.4 (s). Anal. calcd. for $C_{24}H_{42}I_2HfN_2P_2Si_4$: C 29.87, H 4.39, N 2.90; found: C 30.02, H 4.43, N 2.89.

Attempted synthesis of $\{[P_2N_2]Hf\}_2(\mu\text{-}\eta^2\text{:}\eta^2\text{-}N_2)$ (4)

C_8K (0.33 g, 3.32 mmol) and $[P_2N_2]HfI_2$ (**3**) (1.21 g, 1.26 mmol) were each weighed into a 200 mL thick-walled reactor, to which 50 mL of toluene was added, all in the glovebox. The reactor was removed from the glovebox and cooled to –198 °C in a liquid nitrogen bath while under a flow of N_2. After allowing 30 min for equilibration, the reactor was sealed and allowed to warm to room temperature. Following 16 h of stirring, a blue-purple color was observed. The reactor was then allowed to stir vigorously for another 7 days. The solution was then filtered through Celite and evaporated to dryness. Washing with a minimal amount of hexanes (2 × 10 mL) yielded 0.85 g of a dark solid. $^{31}P\{^1H\}$ NMR indicates the composition of this solid to be approximately 52% **4**, 19% **3**, 16% **2**, and 13% **5**. EI-MS: 1450 ($[M]^+$).

Synthesis of $[P_2N_2]HfMe_2$ (6)

To a solution of $[P_2N_2]HfCl_2$ (**1**) (3.02 g, 3.86 mmol) in THF was added 3.0 mol L^{-1} MeMgCl in THF (2.57 mL, 7.77 mmol) at 0 °C. The solution was warmed to room temperature and stirred for 1 h, after which the solvents were evaporated in vacuo. The off-white residue was extracted into toluene (2 × 20 mL) and filtered through celite. The filtrate was evaporated to dryness, and the residue was washed with hexanes (2 × 10 mL), yielding **6** (2.24 g, 77%) as a white powder. The product was crystallized by the slow evaporation of a DME solution.

^1H NMR (C_6D_6, 25 °C, 500.135 MHz) δ: 7.62 (m, 4H, *o*-H phenyl), 7.07 (m, 6H, *m*/*p*-H phenyl), 1.03 (m, 8H, CH_2 ring), 0.72 (t, 6H, Zr-CH_3), 0.22 (s, 12H, $SiMe_2$ ring), 0.20 (s, 12H, $SiMe_2$ ring). $^{31}P\{^1H\}$ (C_6D_6, 25 °C, 202.458 MHz) δ: –9.6 (s). Anal. calcd. for $C_{26}H_{48}HfN_2P_2Si_4$: C 42.12, H 6.53, N 3.78; found: C 42.14, H 6.52, N 3.74.

Synthesis of $\{[P_2N_2]Hf\}_2(\mu\text{-}H_4)$ (7)

Fifty millilitres of C_6H_6 was added to 1.02 g (1.3 mmol) of $[P_2N_2]HfMe_2$ (**6**) in a reactor, which was sealed. The reactor was "freeze–pump–thawed" three times to remove all gases. H_2 was introduced to the reactor, which was cooled to –198 °C. After the solvent had thawed, but prior to warming to room temperature, the reactor was shaken to promote dissolution of H_2 in the solution. The reactor was left overnight, during which time a microcrystalline yellow solid precipitated. This solid was collected on a frit, yielding **7** (0.345 g, 37.2%).

^1H NMR (C_6D_6, 25 °C, 500.135 MHz) δ: 9.07 (quintet, $^2J_{HP}$ = 4.43 Hz, 4H, Hf-H), 7.19 (m, 8H, *o*-H phenyl), 7.12 (m, 12H, *m*/*p*-H phenyl), 0.83 (m, 16H, CH_2 ring), 0.04 (s, 24H, $SiMe_2$ ring), –0.03 (s, 24H, $SiMe_2$ ring). $^{31}P\{^1H\}$ (C_6D_6, 25 °C, 202.458 MHz) δ: 4.4 (s). Anal. calcd. for $C_{48}H_{88}HfN_2P_2Si_4$: C 40.41, H 6.22, N 3.93; found: C 40.56, H 6.21, N 3.76.

Acknowledgements

The authors thank the Natural Sciences and Engineering Research Council of Canada (NSERC) for funding (Discovery Grant to M.D.F.), Mr. Marshall Lapawa for mass spectrometry, and Mr. Peter Borda for elemental analyses.

References

1. M.D. Fryzuk and S.A. Johnson. Coord. Chem. Rev. **200–202**, 379 (2000).
2. D.M. Roddick, M.D. Fryzuk, P.F. Seidler, G.L. Hillhouse, and J.E. Bercaw. Organometallics, **4**, 97 (1985).
3. M.D. Fryzuk, C. Kozak, P. Mehrkhodavandi, L. Morello, B.O. Patrick, and S. Rettig. J. Am. Chem. Soc. **124**, 516 (2002).
4. M.D. Fryzuk, J.B. Love, S.J. Rettig, and V.G. Young. Science (Washington, D.C.), **275**, 1445 (1997).
5. M.D. Fryzuk, J.B. Love, and S.J. Rettig. Organometallics, **17**, 846 (1998).
6. M.D. Fryzuk, D.B. Leznoff, S.F. Ma, S.J.Rettig, and J.V.G. Young. Organometallics, **17**, 2313 (1998).
7. M.D. Fryzuk, T.S. Haddad, M. Murugesapilla, D.H. McConville, and S.J. Rettig. J. Am. Chem. Soc. **115**, 2782 (1993).
8. M.D. Fryzuk, M. Mylvaganam, M.J. Zawarotko, and L.R. MacGillivray. J. Am. Chem. Soc. **115**, 10 360 (1993).
9. M.D. Fryzuk, S.A. Johnson, and S.J. Rettig. Organometallics. **18**, 4059 (1999).
10. M.D. Fryzuk, P.A. Macneil, S.J. Rettig, A.S. Secco, and J. Trotter. Organometallics, **1**, 918 (1982).
11. M.D. Fryzuk, T.S. Haddad, and D.J. Berg. Coord. Chem. Rev. **99**, 137 (1990).
12. M.D. Fryzuk and A. Carter. Organometallics, **11**, 469 (1992).
13. D.G. Black, D.C. Swenson, and R.F. Jordan. Organometallics, **12**, 3539 (1995).
14. D.J. Cardin, M.F. Lappert, and C.L. Raston. Chemistry of organo-zirconium and hafnium compounds. Ellis Horwood Limited, West Sussex. 1986. p. 21.
15. D.F. Shriver, P. Atkins, and C.H. Langford. Inorganic chemistry. W.H. Freeman and Company, New York. 1994.
16. G.W. Watt and J.D. Chrisp. Anal. Chem. **24**, 2006 (1952).
17. G.A. Helmut, F.P.D. Sanzo, M.D. Rausch, and P.C. Uden. J. Organomet. Chem. **107**, 257 (1976).
18. G.A. Razuvaev, L.I. Vyshinskaya, and V.P. Mar′in. Dokl. Akad. Nauk SSSR, **225**, 827 (1975).
19. G.A. Razuvaev, V.P. Mar′in, O.N. Drushkov, and L.I. Vyshinskaya. J. Organomet. Chem. **231**, 125 (1982).
20. D.M. Roddick and J.E. Bercaw. Chem. Ber. **122**, 1579 (1989).
21. J.E. Bercaw and J.R. Moss. Organometallics, **11**, 639 (1992).
22. M.D. Fryzuk, S.J. Rettig, A. Westerhaus, and H.D. Williams. Inorg. Chem. **24**, 4316 (1985).
23. J.E. Gozum and G.S. Girolami. J. Am. Chem. Soc. **113**, 3829 (1991).
24. J.E. Gozum, S.R. Wilson, and G.S. Girolami. J. Am. Chem. Soc. **114**, 9483 (1992).
25. A.B. PangBorn, M.A. Giardello, R.H. Grubbs, R.K. Rosen, and F.J. Timmers. Oganometallics, **15**, 1518 (1996).
26. L.E. Manzer. Inorg. Chem. **21**, 135 (1982).
27. M.D. Fryzuk, J.B. Love, and S.J. Rettig. J. Chem. Soc. Chem. Commun. 2783 (1996).
28. D.E. Bergbreiter and J.M. Killough. J. Am. Chem. Soc. **100**, 2126 (1978).

Appendix A. X-ray crystallographic analysis of $[P_2N_2]HfCl_2$ (1).

Table A1. Crystal data.

Empirical formula	$C_{24}H_{42}N_2Cl_2HfP_2Si_4$
Formula weight	782.29
Temperature (K)	173
Crystal color, habit	Clear, chip
Crystal dimensions (mm)	0.15 × 0.15 × 0.15
Crystal system	Orthorhombic
Lattice type	Primitive
Lattice parameters	
a (Å)	9.3152(8)
b (Å)	16.5962(5)
c (Å)	21.3811(7)
V (Å^3)	3305.5(2)
Space group	$P2_12_12_1$ (#19)
Z value	4
D_{calcd} (g cm^{-3})	1.572
F_{000}	1568.00
μ (cm^{-1}) (Mo Kα)	35.71

Table A2. Intensity measurements.

Diffractometer	Rigaku/ADSC CCD
Radiation	Mo Kα (λ = 0.71069 Å) Graphite monochromated
Detector aperture (mm)	94 × 94
Data images	464 exposures @ 35.0 s
ϕ Oscillation range (χ = 0) (°)	0.0–190.0
ω Oscillation range (χ = 90.0) (°)	–19.0 to 23.0
Detector position (mm)	40.62
Detector swing angle (°)	–5.55
$2\theta_{max}$ (°)	55.8
No. of reflections measured	Total: 28 469 Unique: 3999 (R_{int} = 0.066)
Corrections	Lorentz-polarization Absorption
Trans. factors	0.7796–1.0000

Table A3. Structure solution and refinement.

Structure solution	Patterson methods (DIRDIF92 PATTY)
Refinement	Full-matrix least-squares
Function minimized	$\Sigma\omega(\lvert F_o^2\rvert - \lvert F_c^2\rvert)^2$
Least squares weights	$\omega = 1/[\sigma^2(F_o^2)]$
p-factor	0.0000
Anomalous dispersion	All non-hydrogen atoms
No. observations ($I > 0.00\sigma(I)$)	6846
No. variables	316
Reflection:parameter ratio	21.66
Residuals (on F^2, all data) R; Rw	0.036; 0.055
Goodness of fit indicator	0.51
Max shift/error in final cycle	0.00
No. observations ($I > 3\sigma(I)$)	5913
Residuals (on F, $I > 3\sigma(I)$) R; Rw	0.020; 0.025
Max peak in final difference map (e Å^{-3})	0.68
Min peak in final difference map (e Å^{-3})	–1.10

Table A4. Atomic coordinates and B_{eq}.

Atom	x	y	z	B_{eq}
Hf(1)	0.08378(2)	0.97608(1)	0.16637	0.890(4)
Cl(1)	–0.1402(2)	0.94810(10)	0.10928(9)	2.77(3)
Cl(2)	0.0421(2)	0.84100(10)	0.21020(10)	3.97(5)
P(1)	–0.031(10)	1.08273(8)	0.24618(7)	1.10(3)
P(2)	0.2891(2)	0.92249(9)	0.08962(7)	1.38(3)
Si(1)	0.2845(2)	1.06481(9)	0.27779(7)	1.19(3)
Si(2)	0.4049(2)	0.91470(10)	0.22206(7)	1.69(3)
Si(3)	0.2511(2)	1.10590(10)	0.06974(8)	1.72(3)
Si(4)	–0.0373(2)	1.15670(10)	0.11763(8)	1.62(3)
N(1)	0.2724(5)	0.9895(3)	0.2213(2)	1.21(8)
N(2)	0.1025(5)	1.0873(3)	0.1169(2)	1.39(8)
C(1)	0.1310(6)	1.1375(3)	0.2661(3)	1.21(9)
C(2)	0.4056(7)	0.8657(3)	0.1413(3)	1.8(1)
C(3)	0.3793(6)	1.0166(4)	0.0711(3)	2.3(1)
C(4)	–0.1363(6)	1.1472(4)	0.1955(3)	1.7(1)
C(5)	0.4503(6)	1.1290(4)	0.2742(3)	2.4(1)
C(6)	0.2705(7)	1.0193(4)	0.3573(3)	2.3(1)
C(7)	0.3787(8)	0.8358(4)	0.2832(3)	2.9(2)
C(8)	0.5897(8)	0.9541(5)	0.2343(4)	3.6(2)
C(9)	0.1921(9)	1.1226(5)	–0.0131(3)	3.4(2)
C(10)	0.3649(8)	1.1929(4)	0.0946(4)	2.8(2)
C(11)	–0.1725(8)	1.1444(4)	0.0533(3)	2.8(2)
C(12)	0.0260(8)	1.2639(4)	0.1142(3)	2.6(1)
C(13)	–0.1222(5)	1.0671(4)	0.3204(2)	1.4(1)
C(14)	–0.1755(6)	1.1332(4)	0.3539(3)	2.1(1)
C(15)	–0.2378(7)	1.1212(5)	0.4124(3)	2.9(1)
C(16)	–0.2492(9)	1.0448(5)	0.4370(3)	3.4(1)
C(17)	–0.1970(8)	0.9799(6)	0.4043(3)	3.4(2)
C(18)	–0.1333(7)	0.9908(4)	0.3454(3)	2.3(1)
C(19)	0.2695(6)	0.8646(3)	0.0184(3)	1.5(1)
C(20)	0.3915(6)	0.8336(4)	–0.0127(3)	2.0(1)
C(21)	0.3749(7)	0.7831(4)	–0.0635(3)	2.1(1)
C(22)	0.2399(7)	0.7645(4)	–0.0857(3)	2.0(1)
C(23)	0.1195(7)	0.7964(4)	–0.0571(3)	2.3(1)
C(24)	0.1341(6)	0.8465(4)	–0.0049(3)	1.9(1)

Appendix B. X-ray crystallographic analysis of [P_2N_2]HfMe_2 (6).

Table B1. Crystal data.

Empirical formula	$C_{26}H_{48}HfN_2P_2Si_4$
Formula weight	741.46
Temperature (K)	173
Crystal color, habit	Clear, block
Crystal dimensions (mm)	0.30 × 0.30 × 0.10
Crystal system	Monoclinic
Lattice type	Primitive
Lattice Parameters	
a (Å)	11.3209(7)
b (Å)	10.8041(3)
c (Å)	28.1451(9)
V (Å^3)	3441.6(2)
Space group	$P2_1/n$ (#14)
Z value	4
D_{calcd} (g cm^{-3})	1.431
F_{000}	1504.00
μ (cm^{-1}) (Mo Kα)	32.75

Table B2. Intensity measurements.

Diffractometer	Rigaku/ADSC CCD
Radiation	Mo Kα (λ = 0.71069 Å) Graphite monochromated
Detector aperture (mm)	94 × 94
Data images	772 exposures @ 16.0 s
φ Oscillation range (χ = 0) (°)	0.0–189.9
ω Oscillation range (χ = 90.0) (°)	–19.0 to 23.0
Detector position (mm)	40.47(1)
Detector swing angle (°)	–5.52(1)
$2\theta_{max}$ (°)	55.8
No. of reflections measured	Total: 23 903 Unique: 7571 (R_{int} = 0.041)
Corrections	Lorentz-polarization Absorption
Trans. factors	0.6526–1.0000

Table B3. Structure solution and refinement.

Structure solution	Direct methods (SIR97)
Refinement	Full-matrix least-squares
Function minimized	$\Sigma\omega(\lvert F_o^2\rvert - \lvert F_c^2\rvert)^2$
Least squares weights	$\omega = 1/[\sigma^2(F_o^2)]$
p-factor	0.0000
Anomalous dispersion	All non-hydrogen atoms
No. observations ($I > 0.00\sigma(I)$)	7219
No. variables	316
Reflection:parameter ratio	22.84
Residuals (on F^2, all data) *R*; *Rw*	0.048; 0.107
Goodness of fit indicator	1.47
Max shift/error in final cycle	0.06
No. observations ($I > 3\sigma(I)$)	6957
Residuals (on *F*, $I > 3\sigma(I)$) *R*; *Rw*	0.036; 0.063
Max peak in final difference map (e Å^{-3})	1.35
Min peak in final difference map (e Å^{-3})	–1.37

Table B4. Atomic coordinates and B_{eq}.

Atom	*x*	*y*	*z*	B_{eq}
Hf(1)	0.65750(1)	0.23340(1)	0.65160(5)	1.428(4)
P(1)	0.50370(1)	0.03890(9)	0.63100(4)	1.93(2)
P(2)	0.74380(9)	0.43630(9)	0.60230(3)	1.56(2)
Si(1)	0.38980(1)	0.28500(1)	0.59870(5)	2.14(2)
Si(2)	0.73980(1)	–0.03330(1)	0.60430(5)	2.23(2)
Si(3)	0.79260(1)	0.19670(1)	0.54750(4)	1.87(2)
Si(4)	0.51990(1)	0.50130(1)	0.64240(5)	2.51(3)
N(1)	0.51010(3)	0.34560(3)	0.62890(1)	1.78(7)
N(2)	0.73090(3)	0.12540(3)	0.59540(1)	1.92(7)
C(1)	0.42520(4)	0.11840(4)	0.58290(1)	2.36(9)
C(2)	0.58270(4)	–0.09030(4)	0.60400(2)	2.45(9)
C(3)	0.73360(3)	0.36020(4)	0.54440(1)	1.91(8)
C(4)	0.63670(4)	0.56280(4)	0.60220(2)	3.0(1)
C(5)	0.36070(6)	0.36310(6)	0.53980(2)	4.6(1)
C(6)	0.25150(5)	0.29060(6)	0.63280(3)	4.1(1)
C(7)	0.80190(5)	–0.06790(5)	0.66420(2)	4.1(1)
C(8)	0.82610(5)	–0.12370(5)	0.56060(3)	4.9(2)
C(9)	0.74710(5)	0.12780(5)	0.48850(2)	3.9(1)
C(10)	0.95660(5)	0.20020(5)	0.55270(2)	3.5(1)
C(11)	0.57740(6)	0.52430(6)	0.70410(2)	4.7(1)
C(12)	0.38170(6)	0.59320(5)	0.63480(3)	4.9(2)
C(13)	0.39430(4)	–0.03090(4)	0.66870(2)	2.44(9)
C(14)	0.27350(4)	–0.02800(5)	0.65940(2)	3.5(1)
C(15)	0.19700(5)	–0.08220(7)	0.69140(2)	4.8(2)
C(16)	0.23790(6)	–0.14090(7)	0.73160(2)	4.9(2)
C(17)	0.35790(5)	–0.14420(7)	0.74110(2)	4.8(2)
C(18)	0.43600(4)	–0.08990(5)	0.70970(2)	3.4(1)
C(19)	0.88480(3)	0.51510(4)	0.60590(1)	1.76(8)
C(20)	0.95490(4)	0.53830(5)	0.56660(2)	2.8(1)
C(21)	1.05610(5)	0.60970(5)	0.57160(2)	3.4(1)
C(22)	1.08800(4)	0.66040(5)	0.61520(2)	2.7(1)
C(23)	1.02030(5)	0.63620(5)	0.65420(2)	3.3(1)
C(24)	0.92130(4)	0.56220(5)	0.64960(2)	3.2(1)
C(25)	0.59360(5)	0.19070(5)	0.72540(2)	3.5(1)
C(26)	0.83120(5)	0.26530(5)	0.69210(2)	3.6(1)